



Exacta

ISSN: 1678-5428

exacta@uninove.br

Universidade Nove de Julho

Brasil

Rambo, Carlos Renato; Accordi Junkes, Janaína; Sieber, Heino; Hotza, Dachamir

Biomorphous ceramics as porous supports for zeolite coating

Exacta, vol. 4, núm. 2, 2006, pp. 297-308

Universidade Nove de Julho

São Paulo, Brasil

Disponível em: <http://www.redalyc.org/articulo.oa?id=81040209>

- Como citar este artigo
- Número completo
- Mais artigos
- Home da revista no Redalyc

redalyc.org

Sistema de Informação Científica

Rede de Revistas Científicas da América Latina, Caribe, Espanha e Portugal

Projeto acadêmico sem fins lucrativos desenvolvido no âmbito da iniciativa Acesso Aberto

# Biomorphous ceramics as porous supports for zeolite coating<sup>1</sup>

Carlos Renato Rambo  
UFSC, Florianópolis – SC [Brasil]  
rambo@enq.ufsc.br

Janaína Accordi Junkes  
UFSC, Florianópolis – SC [Brasil]

Heino Sieber  
UFSC, Florianópolis – SC [Brasil]

Dachamir Hotza  
UFSC, Florianópolis – SC [Brasil]

Biotemplating is the processing of microcellular ceramics by reproduction of natural morphologies, where the microstructural features of the biotemplate are maintained in the biomorphic ceramic. Different biotemplates with distinct pore anatomies were used to produce biomorphic supports for the zeolite coating: wood, cardboard, sea-sponge and sisal. The biomorphic ceramics were produced by distinguished processing routes: Al-gas infiltration-reaction, liquid-metal infiltration, dip-coating and sol-gel synthesis, in order to produce nitrides, carbides and oxides, depending on the processing conditions. The zeolite coating was performed by hydrothermal growth of MFI-type (Silicalite-1 and ZSM-5) zeolite crystals onto the internal pore walls of the biomorphic templates. The final biomorphic ceramic-zeolite composites were physically characterized, evaluated in terms of their gas adsorption capabilities and correlated to their microstructure and specific pore anatomy. The combination of the properties of the biomorphic ceramics with the adsorption properties of zeolites results in materials with distinct properties as potential candidates for adsorption and catalytic applications due to their characteristic porosity, molecular sieving capabilities and high thermo-mechanical strength.

**Key words:** Biotemplating. Coating. Porous ceramics. Zeolite ZSM-5.



## 1 Introduction

According to next step.

### 1.1 Biotemplating

Bioinspired ceramics have attained special interest due to their peculiar anatomical features, like the hierarchical cellular morphology and the oriented pore structure (HEUER, 1992; BYRNE; NAGLE, 1997). During the last decades several studies have been focused on the synthesis of this class of materials by different routes (GREIL, 2001). The main innovative feature of this methodology is the possibility to design macro and microporous devices, which could not be produced by conventional techniques.

Biotemplating techniques have been extensively investigated, in order to achieve higher degree of reproduction of the natural tissue. The conversion of native tissues into biomorphic ceramics with hierarchical, microcellular morphology is based on two processing approaches: substitution and transformation. Substitution is achieved by coating the inner surfaces of the plant tissue with oxidic precursors (RAMBO; CAO; SIEBER, 2004; RAMBO et al., 2005; CAO; RAMBO, 2004; OTA et al., 2000; SIEBER et al., 2002b; PATEL; PADHI, 1993). Burning the template in air releases carbon as CO/CO<sub>2</sub> and promotes its consolidation into an oxide ceramic. Transformation involves the direct conversion of the carbonized template by reaction into carbide phases (GREIL; LIFKA; KAINDL, 1998; VOGLI et al., 2001; SIEBER et al., 2002a; VOGLI, SIEBER; GREIL, 2002; RAMBO; MARTINELLI, 2001; OTA et al., 1995).

### 1.2 Zeolites

Zeolites are basically aluminosilicate crystalline structures, which exhibit a well-defined nanopore network, a large surface area and ion-

exchange properties (ACKLEY; REGE; SAXENA, 2003). Zeolites are widely employed in several technological applications as catalyst in organic synthesis, petroleum refining and petrochemical industries.

Commercial ZSM-5 is produced from commercial silica sources in the form of gel, sol and amorphous fumed silica. However, waste materials with high silica content such as rice husk ash and fly ash are potential silica sources for zeolite synthesis. Previous studies (RAWTANI; RAO; GOKHALE, 1989; HAMDAN et al., 1997; RAMLI; LISTIORINI; HAMDAN, 1996; PRAMOD; RAO; GOKHALE, 1981) reported the synthesis of zeolites A, Y, ZSM-5, mordenite, and zeolite beta from rice husk derived silica. In all cases, the silica of the rice husk ash was in amorphous form obtained either by extraction of the silica from the crystalline rice husk ash or by controlled burning of the rice husk.

Zeolite-coated structured composites are widely investigated for several applications, including gas separation and catalysis. Kusakabe and collaborators (1997) studied the formation of a Y-type zeolite membrane on a porous  $\alpha$ -Al<sub>2</sub>O<sub>3</sub> tube for gas separation. Li and collaborators (2005) demonstrated the superior performance of zeolite-based catalysts in the reduction of nitrogen oxides. Buciuman and Kraushaar-Czarnetzki (2001) produced ceramic foam supported nanocrystalline zeolite catalysts. Patcas and collaborators (2005) investigated the methanol-to-olefins conversion over zeolite-coated Al<sub>2</sub>O<sub>3</sub>/Mullite open cell foams.

The combination of structural and morphological properties of biomorphic ceramics with the high specific surface area of zeolites may result in a composite material with unique properties, which might be useful as sensors, catalyst, adsorption and separation devices.

The present work proposes the in situ zeolite synthesis and coating on biomorphic ceramic supports produced by distinguished processing routes and different biotemplates with distinct pore anatomies: wood, cardboard and natural cellulosic sponge. The zeolite coating will be performed by hydrothermal growth of MFI-type (ZSM-5) zeolite crystals onto the internal pore walls of the biomorphic templates.

## 2 Experimental

Three different biotemplates were used as starting materials and three different processing routes were used for the manufacturing of porous ceramics. The processing route was applied according to the initial macroporosity of the template and its pore size and morphology and processing feasibility.

### 2.1 Al<sub>2</sub>O<sub>3</sub> from rattan

As biological templates for manufacturing of the highly porous, biomorphous Al<sub>2</sub>O<sub>3</sub> dried rattan (subfamily *Calamoideae* of the family *Areaceae*) plants were used. The *in natura* samples were cut in discs of approximately 2 centimeters (cm) (rattan) of diameter and 1 cm of height, dried (130° C/2 hour [h] in air) and pyrolysed at 800° C for one hour in N<sub>2</sub> atmosphere in order to decompose the polyaromatic hydrocarbon polymers into carbon (C<sub>B</sub>). In contrast to wood, rattan is a tropical climbing palm that exhibits no branches or seasonal rings (UHL; DRANSFIELD, 1987). It is characterized by a homogeneous profile and vessel distribution. Large vessels (200-330 micrometers [μm]) from the meta-xylem characteristic from this plant, as well as the middle sized cells (around 90 μm) from the phloem are normally found. Subsequently, the carbonized preforms were disposed above an Al-powder bed (*Alfa Aesar*, – 325 mesh,

purity 99.5%) in an Al<sub>2</sub>O<sub>3</sub>-crucible without contact to the powder. The system was placed in a conventional tube furnace and submitted to an Al-vapour phase infiltration process at 1600° C for one hour under vacuum (1-0.1 Pa) for reaction of the carbonized specimens into Al<sub>4</sub>C<sub>3</sub>. After the pyrolysis, the specimens were oxidized and sintered at temperatures between 1,550 and 1,700° C in air for three hours, which resulted in samples with different porosities. Details of the Al infiltration process is described elsewhere (RAMBO; SIEBER, 2005; RAMBO et al., 2006).

### 2.2 TiO<sub>2</sub> from cellulosic sponge

A sol-gel infiltration process of low viscous TiO<sub>2</sub> precursor into a natural cellulose-based polymer sponge, which exhibits a 3D porous network structure (*Luffa aegyptiaca*) was applied. After burn out of the biological preform during sintering process, a porous TiO<sub>2</sub> ceramic was obtained. Low viscous, stable TiO<sub>2</sub>-sol was prepared for the infiltration process. Titania sol was obtained by modification of titanium iso-propoxide (TTiP, Ti [OCH (CH<sub>3</sub>)<sub>2</sub>]<sub>4</sub>, 97%, *Alfa Aesar*) with acetic acid (HOAc, 96%, *Alfa Aesar*) and subsequent hydrolysis in distilled H<sub>2</sub>O. Infiltrated samples were dried in air at 130° C for two hours to form oxide gels in situ. This procedure was repeated up to three times to increase the precursor content in the native sponge. Finally the samples were annealed in air to remove the biopolymer by oxidation and to increase the density of the TiO<sub>2</sub>-struts by sintering at 1,200° C for 1 h. This process is well described elsewhere (CAO; RAMBO; SIEBER, 2004).

### 2.3 SiAlON/SiC from cardboard

Preforms of corrugated cardboard made of secondary cellulose fibers were used as templates (190TL, Wellpappenwerk, Bruchsal / Germany) were dried at 70° C and infiltrated by dip-coating

with a metal powder / preceramic polymer slurry. The slurry was prepared with isopropyl alcohol containing 40 vol. % Si-powder (> 98%), 40 vol. % Al-powder (> 99%) and 20 vol. % of a preceramic polymer (Polymethylsilsesquioxan – PMS, MK, Wacker AG, Burghausen / Germany). The PMS is characterized by a high ceramic yield (Si-C-O) of more than 75 wt.% of SiO<sub>2</sub>, SiC and C in the inorganic residue upon pyrolysis in Ar atmosphere (GREIL, 2000; RAMBO; SIEBER, 2006; SCHEFFLER et al., 2000). The Al/Si ratio corresponds to a weight fraction of 53.8 wt% Al and 46.2 wt% Si, which exhibits a melting temperature of 1,012° C. After dip coating, the specimens were pyrolysed in Ar atmosphere at 1,200° C for one hour. At temperatures above 1,012° C the Si/Al powder mixture forms an alloy melt, which infiltrates the porous carbon. Subsequently, the samples were oxidized in air at 800° C for one hour to increase the amount of oxygen, which is necessary for the  $\beta$  solid solution formation and then submitted to nitridation in N<sub>2</sub> atmosphere at 1,530° C, as described in (RAMBO; SIEBER, 2006).

## 2.4 Zeolite coating

MFI-type zeolites were hydrothermally synthesized, following the procedure described in the literature (ZAMPIERI et al., 2006; RAMLI; BAHRUJI, 2003; VAN GRIEKEN, 2000; GARCIA-MARTINEZ, 2001). The reagents used for the synthesis in a distilled water solution were: tetraprylamonium bromide TPABr, (Fluka, 98%), sodium aluminate Na. AlO<sub>2</sub>, (Riedel), sodium hydroxide P. A. – NaOH (Vetec, 97%) and silica obtained from rice husk with 98.3% purity.

The reagents were mixed and placed in a Teflon crucible containing the biomorphic support. The reactional system was then kept for seven days in an autoclave at 150° C. Afterwards, the coated samples were washed in distilled water, dried and

calcined in air at 550° C for five hours to remove the organic template.

The zeolite synthesis and coating was performed in situ on the biomorphic substrates, in order to optimize the adsorption properties, permeability and specific surface area, as shown by Zampieri and collaborators (ZAMPIERI et al., 2006) in biomorphic SiSiC composites coated with MFI-type zeolites.

The conventional mechanism proposed for the zeolite synthesis is a two-step process: nucleation, where crystalline seeds for the zeolite are formed, and crystal grown (VAN GRIEKEN, 2002).

The schematic diagram of Figure 1 describes the experimental methodology used for the synthe-

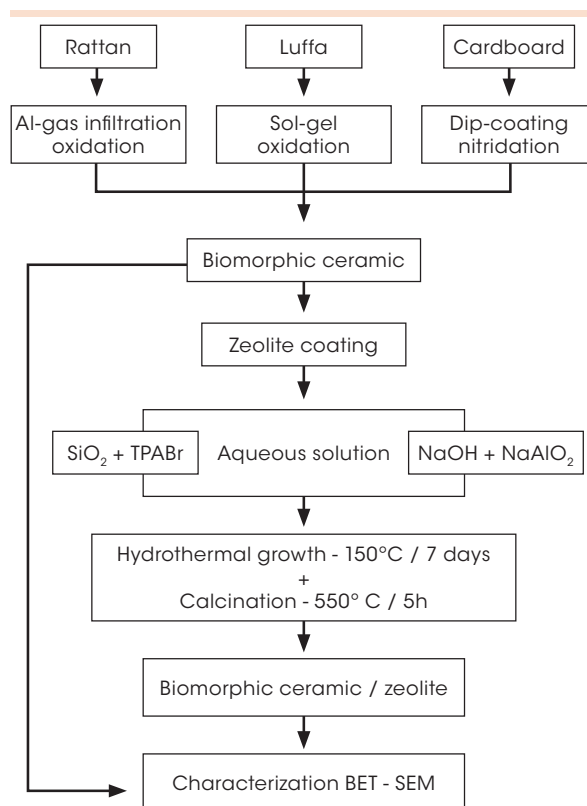


**Figure 1: Schematic diagram of the manufacturing of biomorphous ceramic from cellulose-based template structures and coating with MFI-type zeolites**

Source: The authors.

sis of the biomorphic substrates and their ZSM-5 zeolite coating.

The phase composition of the ceramic products was determined by X-ray diffractometry, XRD (Philips, X'Pert) working with monochromated  $\text{CuK}_\alpha$  radiation. The microstructure was characterized by scanning electron microscopy, SEM (Philips, XL-30). The skeleton density was measured by helium pycnometry (Micromeritics, Accu Pyk 1330). The open porosity was estimated by the relation between the skeleton and the geometrical densities. Specific surface area was determined by  $\text{N}_2$  adsorption isotherms using the B. E. T. method<sup>2</sup> (Quantachrome, Autosorb).

### 3 Results and discussion

Figure 2 shows the XRD spectra of the produced ceramic templates. All unassigned diffraction peaks in Figure 2 are related to the main phases. The cellular ceramic produced from cardboard is composed of  $\beta$ -SiAlON and  $\beta$ -SiC, with a residual  $\text{Si}_3\text{N}_4$  phase (spectrum a).

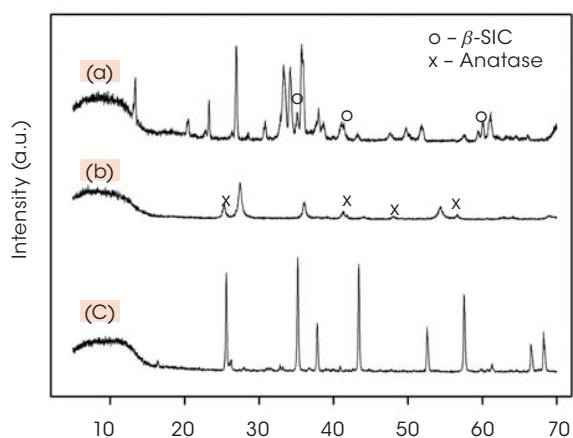


**Figure 2:** X-ray diffractograms of the obtained biomorphic ceramics: a) SiAlON/SiC composite from cardboard; b)  $\text{TiO}_2$  from cellulosic sponge and c)  $\text{Al}_2\text{O}_3$  from rattan

Source: The authors.

A more detailed analysis on the phase evolution during nitridation can be found in previous publication (RAMBO; SIEBER, 2006). The biomorphic  $\text{TiO}_2$  is composed mainly by rutile, with anatase as secondary phase (spectrum b). Finally, in the spectrum c, only  $\alpha$ - $\text{Al}_2\text{O}_3$  was detected in the biomorphic ceramic produced from rattan.

After the hydrothermal process and subsequent calcination, MFI-type zeolite was formed.

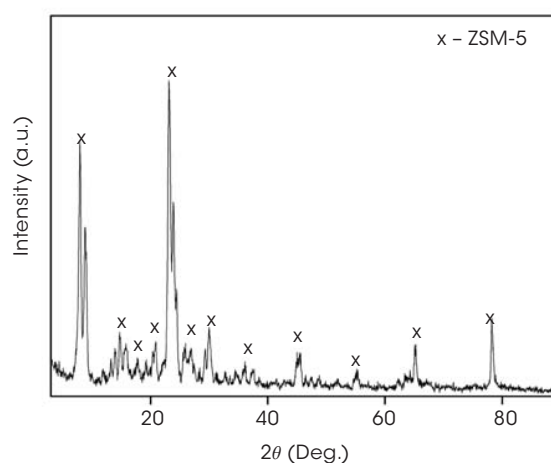


**Figure 3:** X-ray diffractogram of the zeolite powder after the hydrothermal synthesis and calcinations

Source: The authors.

Figure 3 shows the XRD pattern of the substrate surface after coating.

Only diffraction peaks related to the zeolite ZSM-5 were detected, indicating a full zeolite formation. The synthesized zeolite is expressed by the general formula  $\text{H}_{0,32}[\text{Si}_{95,68}\text{Al}_{0,32}\text{O}_{192}]$  and belongs to the spatial group  $\text{P}12_1/\text{n}1$ .

The microstructure of the composites, as well as the quality of the zeolite coating, e. g. the homogeneity of the coating was evaluated by SEM observations. Figures 4, 5 and 6 show the SEM micrographs of the biomorphic ceramics before and after the zeolite coating.

The original template anatomical features were maintained after the biotemplating process,



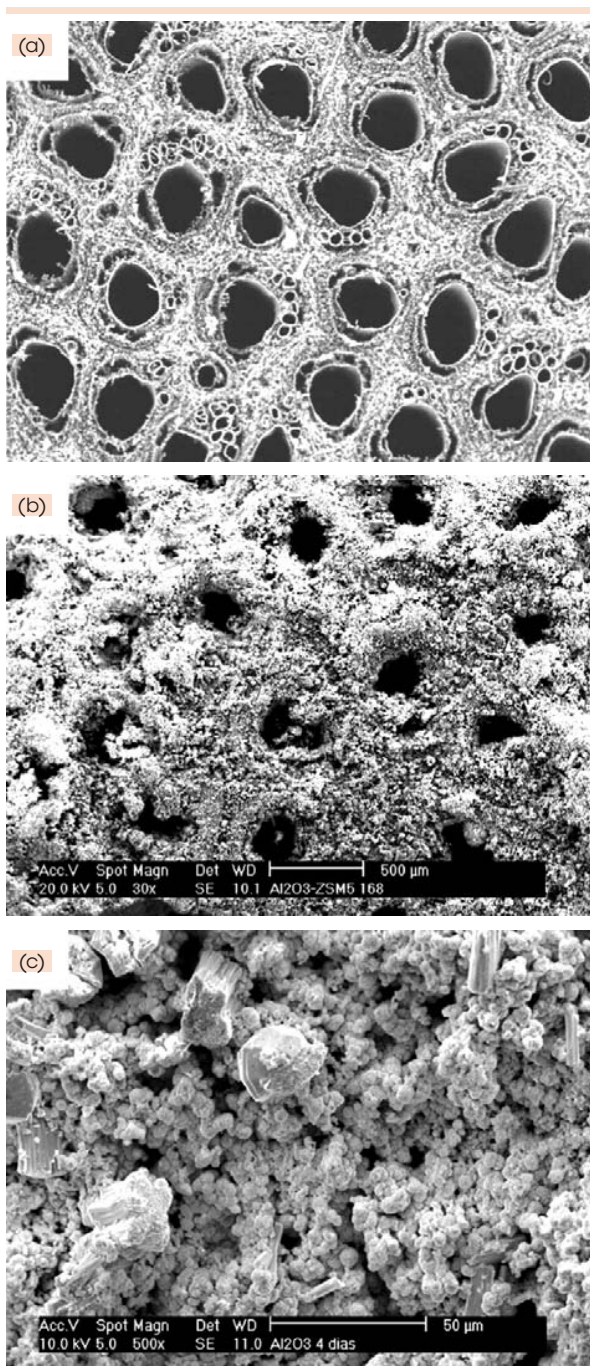


**Figure 4: SEM micrographs of the biomorphic  $\text{Al}_2\text{O}_3$ -support produced from rattan. a) Biomorphic  $\text{Al}_2\text{O}_3$ ; b)  $\text{Al}_2\text{O}_3$  coated support and c) Details of the coating zeolite particles**

Source: The authors.

indicating that the three routes were adequately applied for each morphology (Figures 4, 5, 6a). The rattan vessels and the fibrous network structure

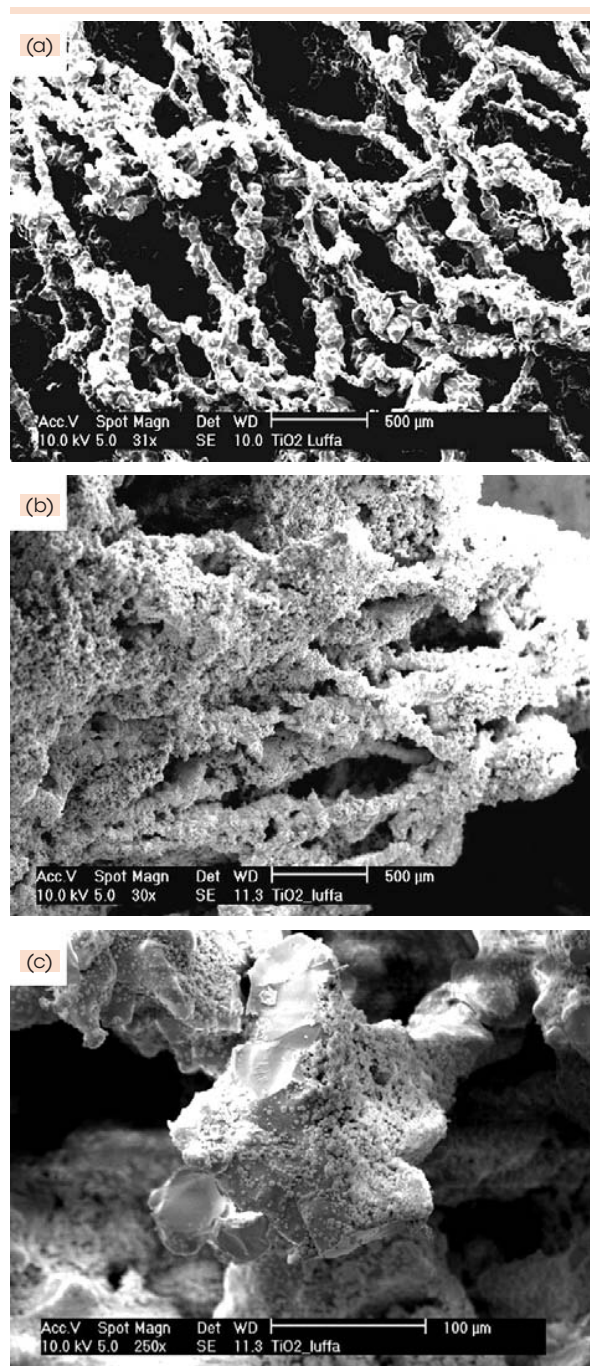


**Figure 5: SEM micrographs of the biomorphic  $\text{TiO}_2$ -support produced from cellulosic sponge (*Luffa*). a) Biomorphic  $\text{TiO}_2$ ; b)  $\text{TiO}_2$  coated support and c) Details of the coating zeolite particles**

Source: The authors.

of the cellulosic sponge were well reproduced in the biomorphic ceramic. The original biotemplate



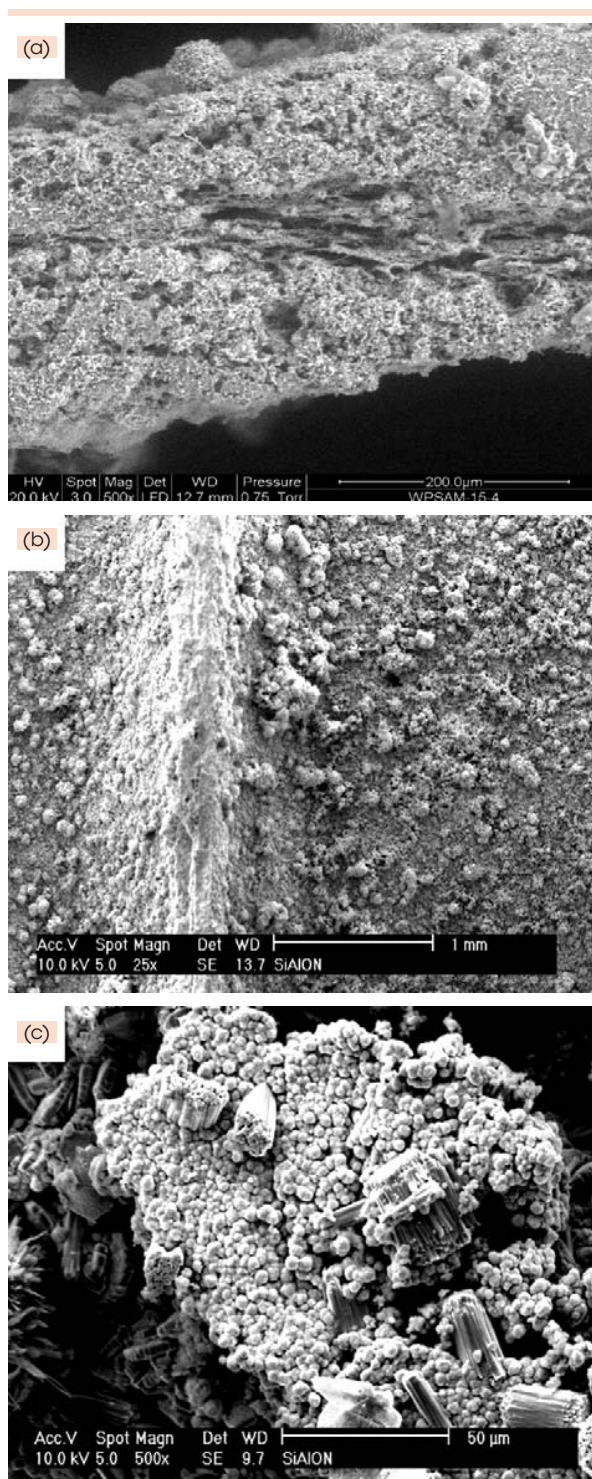


**Figure 6: SEM micrographs of the biomorphic SiAlON/SiC-support produced from cardboard. a) SiAlON/SiC-support; b) SiAlON/SiC coated support and c) Details of the coating zeolite particles**

Source: The authors.

structure as well as a detailed discussion of the microstructure after ceramic conversion is described previously (JONÁŠOVÁ et al., 2004; RAMBO; SIEBER, 2006). After the hydrothermal synthesis, a homogeneous layer formed by zeolite particles was formed on the surface of the substrates (Figs. 4, 5, 6b). The microstructural details of the zeolite particles are shown in Figures 4, 5, 6c. Particles with sizes ranging from 500 nanometers (nm) to 2 μm, common for all substrates, are homogeneously distributed on the substrate surfaces. Figure 5c shows a fractured strut surface of the biomorphic TiO<sub>2</sub>, evidencing the TiO<sub>2</sub> grains which form the sponge struts.

Cellular 3D network structures may provide several advantages, when compared to monolithic honeycomb structures. In catalysis, for example, cellular structures offer in addition to the low pressure drop the advantage of a turbulent flow enhancing the mass and heat transfer between the fluid phase and the catalyst washcoat, and they also allow radial mixing (BUCIUMAN; KRAUSHAAR-CZARNETZKI, 2001).

The N<sub>2</sub> adsorption isotherms are shown in Figure 7. Basically, isotherms of type IV characterize the biomorphic ceramic supports, as well as the zeolite coated supports. Type IV is typical of multilayer physical adsorption, combined with capillary adsorption in pores (REED, 1995; BEYEA, 2003). The existence of hysteresis indicates the presence of mesopores (pore width between 2 and 50 nm) adsorbing and desorbing by capillary condensation and evaporation, respectively, and arises from the faster desorption, compared to adsorption, at higher P/P<sub>0</sub> values (> 0.5).

In such isotherms the thickness of the adsorbed layer increases with the increase of N<sub>2</sub> pressure, with more N<sub>2</sub> adsorbed on materials of higher surface area for a given pressure. When the temperature is below the critical point and the pores are greater than a few times the molecular



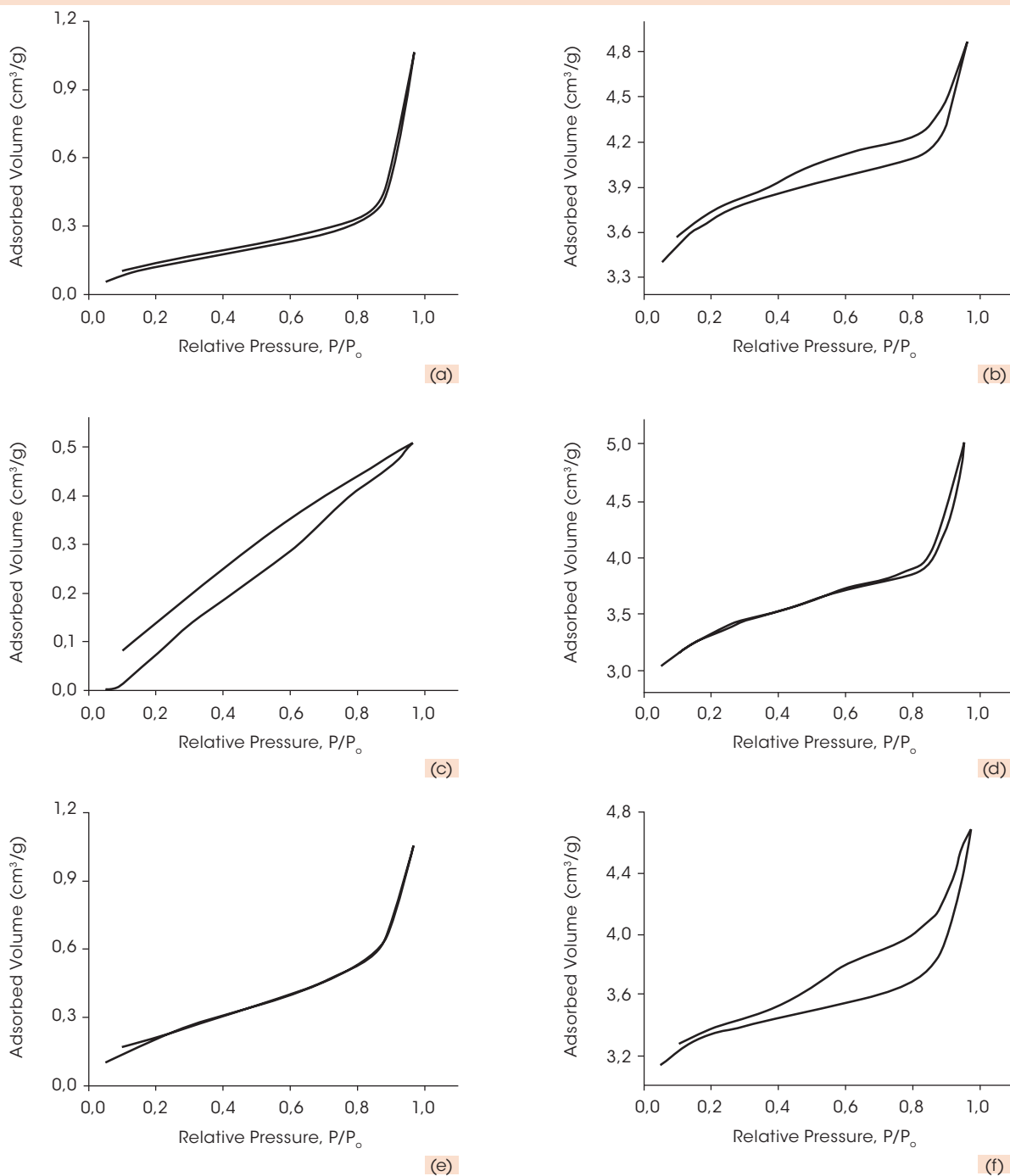


**Figure 7:  $N_2$  adsorption/desorption isotherms of: a)  $\text{Al}_2\text{O}_3$  from rattan; c)  $\text{TiO}_2$  from cellulosic sponge and e)  $\text{SiAlON/SiC}$  composite from cardboard. The respective zeolite coated biomorphic supports are displayed on the right**

Source: The authors.

diameter of the adsorbate, the adsorbate fills the entire pore according to a phenomenon known as capillary condensation. Such condensation transi-

tions are observed in the isotherm as a steep rise in the amount of gas adsorbed at the capillary condensation pressure. Since the vapour pressure of a

wetting fluid is lower over a film of higher curvature, the capillary condensation pressure is then a function of the pore size, related by the Kelvin equation (GLASS; GREEN, 1999).

During desorption, the capillary evaporation pressure is often lower than the condensation pressure, leading to an adsorption/desorption hysteresis loop the shape of which is determined by the pore morphology (REED, 1995). Differences in the individual isotherms in Figure 7 therefore reflect differences in the local surface area, porosity, morphology, surface chemistry, and pore size (GREGG; SING, 1982; LOWELL; SHIELDS, 1991).

N<sub>2</sub> sorption isotherm measurements contain information about many different microstructural parameters. BET theory is a kinetic theory for multilayer adsorption of gases in porous solids, the use of which permits determination of the specific surface area of materials by calculation of the monolayer capacity N<sub>m</sub> from the adsorption isotherm. Using BET theory (within the range of 0.05 < P/P<sub>0</sub> < 0.4) it is possible to linearize an adsorption isotherm by plotting:

$$1/W (P_0/P - 1) \text{ vs } P/P_0 \quad (1)$$

where W is the mass of gas adsorbed for a given equilibrium pressure. The slope m and intercept i of this linearized BET plot then permits calculation of both N<sub>m</sub> and the so-called BET “C value”.

$$N_m = \frac{1}{m + i},$$

$$C = \frac{m}{i} + 1 \quad (2)$$

Surface area S is calculated from the monolayer capacity by the relation:

$$\frac{N_m \Omega \bar{N}}{\bar{M}} \quad (3)$$

where  $\bar{N}$  is the Avogadro number,  $\bar{M}$  is the molecular weight of the adsorbate, and  $\Omega$  is the average cross-sectional area occupied by an adsorbed gas molecule in a completed monolayer. The BET C value is a measure of the strength of adsorbate/substrate interaction, and is related to the net energy of adsorption (q<sup>st</sup>-q<sub>L</sub>) by

$$(q^{st} - q_L) = RT \ln C, \quad (4)$$

	Macroporosity (%)	SSA (m <sup>2</sup> /g)	Micropore volume (cm <sup>3</sup> /g)	Micropore width (Å)
Before coating				
Rattan Al <sub>2</sub> O <sub>3</sub>	89 ± 1	1.75 (5)	< 0.0001	162.3 ± 0.5
Luffa TiO <sub>2</sub>	83 ± 1	1.41 (5)	< 0.0001	434.5 ± 0.5
Cardboard SiAlON/SiC	85 ± 1	1.40 (5)	< 0.0001	149.7 ± 0.5
After coating				
Rattan Al <sub>2</sub> O <sub>3</sub>	84 ± 1	111.40 (5)	0.0406 (5)	53.7 ± 0.5
Luffa TiO <sub>2</sub>	82 ± 1	69.59 (5)	0.0236 (5)	54.8 ± 0.5
Cardboard SiAlON/SiC	85 ± 1	91.40 (5)	0.0373 (5)	47.8 ± 0.5

**Table 1: BET results and calculated overall porosity**

Source: The authors.



where  $q^{\text{st}}$  and  $q_L$  are the isosteric heat of adsorption and molar heat of liquefaction, respectively. Thus, for a given adsorbate, differences in the local C value reflect differences in the underlying energetic properties of the pore walls, affecting the surface chemistry (BEYEA, 2003).

Table 1 summarizes the BET results before and after the zeolite coating. The specific surface area, the micropore width (DR method) and the micropore volume (t-method) are shown. The numbers in parenthesis indicated the error in the last digit.

All coated biomorphic supports exhibit specific surface areas of ~65 times higher than the respective biomorphic ceramics. The small micropore volume of the biomorphic ceramic supports indicates that only the strut or cell wall inherent porosity counts for the specific surface area. After zeolite coating, the micropore width decreased to 25% of the initial value, except for the cellulosic sponge, which decreased to approximately 15%. The macroporosity was not substantially affected by the zeolite coating.

The results for rattan are similar to those obtained by Zampieri and collaborators (ZAMP-IERI et al., 2006), where the specific surface area was  $<1 \text{ m}^2/\text{g}$  and  $163 \text{ m}^2/\text{g}$  for the biomorphic SiSiC and ZSM-5 coated SiSiC, respectively. The biomorphic SiSiC composites exhibit a lower micropore volume than the biomorphic  $\text{Al}_2\text{O}_3$ , due to the obstruction of the micro-vessels and cells of rattan, caused by excess of Si, proceeding from the infiltration process.

## 4 Final considerations

Cellular, biomorphic ceramics were successfully coated in situ with ZSM-5 zeolite by hydrothermal synthesis. SiAlON/SiC-composite was produced from cardboard,  $\text{Al}_2\text{O}_3$  was produced

from rattan and  $\text{TiO}_2$  was produced from natural cellulose sponge. The biomorphic composites exhibited porosities ranging from 82-89%, depending on the original template and specific surface area of  $1.4\text{-}1.8 \text{ cm}^2/\text{g}$ , before coating. After zeolite coating the ceramics exhibited specific surface area 65 times higher, which might be useful as sensors, catalyst, adsorption and separation devices.

## Acknowledgements

The authors thank CNPq-Brazil for the financial support.

## Endnotes

- 1 N. Ed.: Texto originalmente apresentado no Cimtec 2006 (In: INTERNATIONAL CERAMIC CONGRESS, 11., 4-9 jun. 2006, Acireale. *Proceedings...* Acireale: Cimtec, 2006.
- 2 N. Ed.: Em 1938, Stephen Brunauer, Paul Hugh Emmett, and Edward Teller derivaram uma equação para absorção de gases em multicamadas na superfície de sólidos. A equação, chamada BET (anagrama das iniciais das famílias dos cientistas), tem como base a hipótese de que as forças responsáveis pela condensação do gás são as mesmas que atraem as moléculas para a formação de multicamadas.

## References

- ACKLEY, M. W.; REGE, S. U.; SAXENA, H. Application of natural zeolites in the purification and separation of gases. *Microporous and Mesoporous Materials*, v. 61, n. 1-3, p. 25-42, 2003.
- BEYEA, S. D. et al. Nondestructive characterization of nanopore microstructure: spatially resolved Brunauer-Emmett-Teller isotherms using nuclear magnetic resonance imaging. *Journal of Applied Physics*, v. 94, n. 2, p. 935-941, 2003.
- BUCIUMAN, F.-C.; KRAUSHAAR-CZARNETZKI, B. Preparation and characterization of ceramic foam supported nanocrystalline zeolite catalysts. *Catalysis Today*, v. 69, n. 1-4, p. 337-342, 2001.
- BYRNE, C. E.; NAGLE, D. E. Cellulose derived composites: a new method for materials processing. *Materials Research Innovations*, v. 1, n. 3, p. 137-144, 1997.

- CAO, J.; RAMBO, C. R. Preparation of porous  $\text{Al}_2\text{O}_3$ -ceramics by biotemplating of wood. *Journal of Porous Materials*, v. 11, n. 3, p. 163-172, 2004.
- CAO, J.; RAMBO, C. R.; SIEBER, H. Manufacturing of microcellular, biomorphous oxide ceramics from native pine wood. *Ceramics International*, v. 30, no. 7, p. 1.967-1.970, 2004.
- GARCIA-MARTINEZ, J. et al. Synthesis and characterisation of MFI-type zeolites supported on carbon materials. *Microporous and Mesoporous Materials*, v. 42, n. 2-3, p. 255-268, 2001.
- GLASS, S. J.; GREEN, D. J. Permeability and infiltration of partially sintered ceramics. *Journal of the American Ceramic Society*, v. 82, n. 10, p. 2.745-2.752, 1999.
- GREGG, S. J.; SING, K. S. W. *Adsorption, surface area and porosity*. 2. ed. London: Academic Press, 1982.
- GREIL, P. Biomorphous ceramics from lignocellulosics. *Journal of the European Ceramic Society*, v. 21, n. 2, p. 105-118, 2001.
- GREIL, P. Polymer derived engineering ceramics. *Advanced Engineering Materials*, v. 2, n. 6, p. 339-348, 2000.
- GREIL, P.; LIFKA, T.; KAINDL, A. Biomorphic cellular silicon carbide ceramics from wood: I. Processing and microstructure. *Journal of the European Ceramic Society*, v. 18, n. 14, p. 1961-1973, 1998.
- HAMDAN, H. et al.  $^{29}\text{Si}$  MAS NMR, XRD and Fesem studies of the rice husk silica for the synthesis of zeolites. *Journal of Non-Crystalline Solids*, v. 211, p. 126-131, 1997.
- HEUER, A. H. et al. Innovative materials processing strategies: a biomimetic approach. *Science*, v. 255, n. 5.048, p. 1.098-1.105, 1992.
- JONÁŠOVÁ, L. et al. *In-vitro* calcium phosphate formation on cellulose - based materials. *Key Engineering Materials*, v. 254-256, p. 1013-1.016, 2004.
- KUSAKABE, K. et al. Formation of a Y-type zeolite membrane on a porous-alumina tube for gas separation. *Industrial & Engineering Chemistry Research*, v. 36, n. 3, p. 649-655, 1997.
- LI, M. et al. Possible reasons for the superior performance of zeolite-based catalysts in the reduction of nitrogen oxides. *Journal of Catalysis*, v. 235, n. 1, p. 201-208, 2005.
- LOWELL, S.; SHIELDS, J. E. *Powder surface area and porosity*. 3. ed. New York: Chapman & Hall, 1991.
- OTA, T. et al. Biomimetic process for producing SiC wood. *Journal of the American Ceramic Society*, v. 78, n. 12, p. 3.409-3.411, 1995.
- OTA, T. et al. Porous titania ceramic prepared by mimicking silicified wood. *Journal of the American Ceramic Society*, v. 83, n. 6, p. 1.521-1.523, 2000.
- PATCAS, F. C. The methanol-to-olefins conversion over zeolite-coated ceramic foams. *Journal of Catalysis*, v. 231, n. 1, p. 194-200, 2005.
- PATEL, M.; PADHI, B. K. Titania fibers through jute fiber substrates. *Journal of Materials Science Letters*, v. 12, n. 15, p. 1.234-1.235, 1993.
- PRAMOD, K. B.; RAO, M. S.; GOKHALE, K. V. G. K. Synthesis of mordenite type zeolite using silica from rice husk ash. *Industrial & Engineering Chemistry Product Research and Development*, v. 20, p. 721-726, 1981.
- RAMBO, C. R. et al. Biomimetic apatite coating on biomorphous alumina scaffolds. *Materials Science & Engineering C*, v. 26, n. 1, p. 92-99, 2006.
- RAMBO, C. R. et al. Manufacturing of biomorphic (Si, Ti, Zr)-carbide ceramics by sol-gel processing. *Carbon*, v. 43, n. 6, p. 1.174-1.183, 2005.
- RAMBO, C. R.; CAO, J.; SIEBER, H. Preparation and properties of highly porous, biomorphic YSZ ceramics. *Materials Chemistry and Physics*, v. 87, n. 2-3, p. 345-352, 2004.
- RAMBO, C. R.; MARTINELLI, J. R. Synthesis and Characterization of SiC from Bamboo. *Key Engineering Materials*, v. 189-191, p. 9-15, 2001.
- RAMBO, C. R.; SIEBER, H. Manufacturing of cellular  $\beta$ -SiAlON/ $\beta$ -SiC composite ceramics from cardboard. *Journal of Materials Science*, v. 41, p. 3.315-3.322, 2006.
- RAMBO, C. R.; SIEBER, H. Novel synthetic route to biomorphic  $\text{Al}_2\text{O}_3$  ceramics. *Advanced Materials*, v. 17, n. 8, p. 1.088-1.091, 2005.
- RAMLI, Z.; BAHRUJI, H. Synthesis of ZSM-5 type zeolite using crystalline silica of rice husk ash. *Malaysian Journal of Chemistry*, v. 5, n. 1, p. 48-55, 2003.
- RAMLI, Z.; LISTIORINI, E.; HAMDAN, H. Optimization and reactivity study of silica in the synthesis of zeolites from rice husk. *Jurnal Teknologi*, v. 25, p. 27-36, 1996.
- RAWTANI, A. V.; RAO, M. S.; GOKHALE, K. V. G. K. Synthesis of ZSM-5 zeolite using silica from rice husk ash. *Industrial & Engineering Chemistry Research*, v. 28, n. 9, p. 1.411-1.414, 1989.
- REED, J. S. *Principles of ceramic processing*. 2. ed. New York: Wiley-Interscience, 1995.
- SCHEFFLER, M. et al. Pyrolytic decomposition of preceramic organo polysiloxanes. *Ceramic Transactions*, v. 115, p. 239-250, 2000.
- SIEBER, H. et al. CVI-R gas phase processing of porous, biomorphic SiC-ceramics. *Key Engineering Materials*, v. 206-213, n. 3, p. 2.013-2.016, 2002a.





SIEBER, H. et al. Manufacturing of porous oxide ceramics by replication of plant morphologies. *Key Engineering Materials*, v. 206-213, n. 3, p. 2.009-2.012, 2002b.

UHL, N. W.; DRANSFIELD, J. *General Palmarum: a classification of palms based on the work of H. E. Moore Jr. Bailei*. 1. ed. Lawrence: Allen Press, 1987.

VAN GRIEKEN, R. et al. Anomalous crystallization mechanism in the synthesis of nanocrystalline ZSM-5. *Microporous and Mesoporous Materials*, v. 39, p. 135-147, 2000.

VOGLI, E. et al. Conversion of oak to cellular silicon carbide ceramic by gas-phase reaction with silicon monoxide. *Journal of the American Ceramic Society*, v. 84, n. 6, p. 1.236-1.240, 2001.

VOGLI, E.; SIEBER, H.; GREIL, P. Biomorphic SiC-ceramic prepared by Si-vapor phaseinfiltration of wood. *Journal of the European Ceramic Society*, v. 22, n. 14-15, p. 2.663-2.668, 2002.

Recebido em 9 ago. 2006 / aprovado em 11 nov. 2006

**Para referenciar este texto**

RAMBO, C. R. et al. Biomorphous ceramics as porous supports for zeolite coating. *Exacta*, São Paulo, v. 4, n. 2, p. 297-308, jul./dez. 2006.